Supplementary Material:
Emergent Spatial Coordination from Negative Selection Alone

Anonymous

Density Sweep Robustness

The main experiments use a fixed density of 7.5% (30 agents on a 20×20 grid). To assess robustness across density levels, we evaluated both Phase 1 and Phase 2 across 12 density conditions: 3 grid sizes (15×15, 20×20, 30×30) $\times$ 4 agent counts (15, 30, 60, 90), yielding densities from 0.017 to 0.400. Each condition was evaluated with 600 rules (100 rules $\times$ 6 seed batches), totaling 14,400 rule evaluations, all using the Miller-Madow bias-corrected MI estimator.

Table 1 and Figures 1 and 2 present the results. Phase 2 achieves nonzero median $\text{MI}_{\text{excess}}$ in 8 of 12 conditions, including all conditions with ≥ 60 agents, peaking near $d = 0.100$ ($\text{MI}_{\text{excess}} = 0.246$ bits at 30×30, 90 agents) before declining at higher densities. Phase 1 remains at zero median $\text{MI}_{\text{excess}}$ across all 12 conditions, confirming that the Phase 2 advantage is not an artifact of the specific grid configuration used in the main experiments.

Phase 2 also consistently achieves higher survival rates than Phase 1, with the gap widening at higher densities (e.g., 76.7% vs. 64.0% at $d = 0.225$; 83.7% vs. 68.0% at $d = 0.400$).

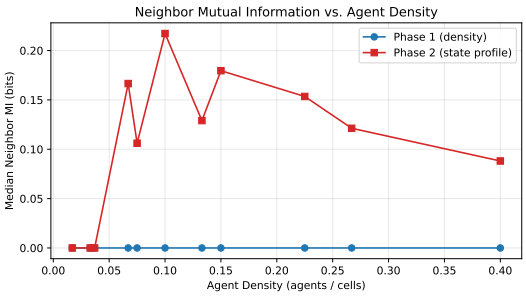

Figure 1: Median neighbor MI vs. agent density for Phase 1 and Phase 2. Phase 2 MI peaks at medium densities and declines at higher densities, while Phase 1 remains at zero throughout.

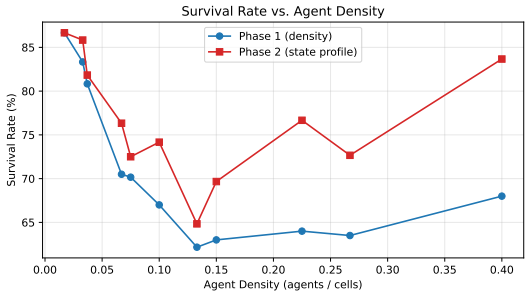

Figure 2: Survival rate vs. agent density. Phase 2 consistently achieves higher survival than Phase 1, with the gap widening at higher densities.

Multi-Seed Robustness

The main experiments evaluate each rule table with a single simulation seed. To assess whether high-$\text{MI}_{\text{excess}}$ rules are robust properties of the rule table rather than seed-specific accidents, we selected the top 50 Phase 2 rules by $\text{MI}_{\text{excess}}$ from the main experiment and re-evaluated each across 20 independent simulation seeds.

Table 2 shows that 82% of top Phase 2 rules maintain positive median $\text{MI}_{\text{excess}}$ across seeds, and on average 73.3% of seeds per rule produce positive excess MI. This confirms that elevated MI in Phase 2 is a robust property of the rule table, not a stochastic artifact of a single initial configuration. The same-state adjacency fraction (a categorical spatial statistic appropriate for nominal state data) is also recorded per seed in the multi-seed dataset and confirms local coordination patterns.

Moran's I by Condition

Table 1 in the main text reports the same-state adjacency fraction as the primary categorical spatial statistic. For completeness, we report Moran's I here, noting that it treats categorical states as numeric (computing deviations from an arithmetic mean) and is therefore inappropriate as a primary indicator for nominal data.

Table 1: Density sweep results across 12 conditions. MI_{excess} values are Miller-Madow corrected, bits. Phase 2 achieves nonzero median MI_{excess} in 8 of 12 conditions, including all conditions with ≥ 60 agents, while Phase 1 remains at zero across all densities tested.

Density	Grid	Agents	Median MI_{excess} (bits)		Survival (%)	
			P1	P2	P1	P2
0.017	30×30	15	0.000	0.000	86.7	86.7
0.033	30×30	30	0.000	0.000	83.3	85.8
0.037	20×20	15	0.000	0.000	80.8	81.8
0.067	15×15	15	0.000	0.000	68.7	76.0
0.067	30×30	60	0.000	0.199	70.5	76.3
0.075	20×20	30	0.000	0.114	70.2	72.5
0.100	30×30	90	0.000	0.246	67.0	74.2
0.133	15×15	30	0.000	0.130	62.2	64.8
0.150	20×20	60	0.000	0.191	63.0	69.7
0.225	20×20	90	0.002	0.176	64.0	76.7
0.267	15×15	60	0.000	0.148	63.5	72.7
0.400	15×15	90	0.000	0.107	68.0	83.7

Table 2: Multi-seed robustness of top-50 Phase 2 rules (20 seeds each).

Metric	Value
Rules with median $MI_{excess} > 0$	41/50 (82.0%)
Mean $P(MI_{excess} > 0)$ across seeds	0.733
Overall survival rate	76.2%

Table 3: Median Moran's I by condition (final-step snapshot, 5,000 rules per condition). Moran's I treats states as numeric and is a secondary indicator; see Table 1 for the categorical adjacency fraction.

Condition	Median Moran's I
Random Walk	-0.030
Control	0.124
Phase 1	-0.011
Phase 2	-0.020

Halt Window Sensitivity

The main experiments use a 10-step halt window. To assess sensitivity, we evaluated the top-50 Phase 2 rules across halt windows of {5, 10, 20} steps.

Table 4: Halt window sensitivity for top-50 Phase 2 rules. Results are qualitatively unchanged across the tested range.

Halt Window	Survival Rate	Median MI_{excess}
5	78.0%	0.486
10	78.0%	0.486
20	78.0%	0.486

Table 4 confirms that the halt-window parameter has no impact on the qualitative findings for these top-performing rules: survival rates (78.0%) and median MI_{excess} (0.486 bits) are identical across all three tested windows. This indicates that the top-50 rules either survive to completion or halt well within the first 5 steps, with no rules in the intermediate regime.

Survival Rates with Confidence Intervals

Random Walk MI_{excess} Across Densities

To confirm that the random walk's MI_{excess} remains near zero regardless of agent density, we extended the density sweep to include the Random Walk condition. Across all 12 density conditions (density range 0.017–0.400), the random walk produces $MI_{excess} \approx 0$ (median ≤ 0.06 bits), confirming that its elevated raw MI is entirely attributable to pair-count bias at all tested densities.

Table 5: Survival rates with Wilson score 95% confidence intervals (5,000 rules per condition).

Condition	Survived / Total	Rate	95% CI
Random Walk	5000/5000	100.0%	[99.9, 100.0]%
Control	2225/5000	44.5%	[43.1, 45.9]%
Phase 1	3570/5000	71.4%	[70.1, 72.6]%
Phase 2	3735/5000	74.7%	[73.5, 75.9]%

Alternative Null Models

In addition to the state-shuffle null used throughout the main text, we evaluated two alternative null models to assess the robustness of the MI calibration:

- Block shuffle: States are shuffled within spatial blocks (4×4), preserving local autocorrelation structure while destroying inter-block correlations.
- Fixed-marginal: Synthetic snapshots are generated with identical marginal state distributions but independent spatial placement (each position draws independently from the observed state frequencies).

Table 6: Alternative null model comparison for top-50 Phase 2 rules (mean MI across 200 null samples per rule). All three null models produce substantially lower MI than the observed values, confirming that Phase 2's elevated MI reflects genuine spatial coordination.

Null Model	Mean Null MI (bits)
State shuffle (main text)	0.264
Block shuffle (4×4)	0.899
Fixed-marginal	0.250

The block-shuffle null produces substantially higher MI (0.899 bits) than the state-shuffle null (0.264 bits), as expected since it preserves within-block correlations. The fixed-marginal null (0.250 bits) is comparable to the state-shuffle. In all cases, mean observed MI for the top-50 Phase 2 rules (1.646 bits) substantially exceeds the null values, confirming genuine spatial coordination.

Spatial Scrambling Control

To confirm that Phase 2's elevated MI depends on agents' specific positions rather than their state distribution alone, we performed spatial scrambling: for each rule's final snapshot, we randomly reassigned occupied positions among agents while keeping their states fixed ($N = 200$ scrambles per rule).

For top-50 Phase 2 rules, the mean observed MI is 1.646 bits while the mean scrambled MI drops to 0.270 bits—comparable to the shuffle null baseline (0.264 bits). This confirms that the observed MI arises from genuine local spatial coordination (agents with correlated states being near each other) rather than from the state distribution itself.

Transfer Entropy

Mutual information measures symmetric statistical dependence between neighboring states. To assess directional information flow, we computed transfer entropy (TE) from neighbor states to agent next-states:

$$\mathrm{TE} = I(S_j^t; S_i^{t+1} \mid S_i^t) \tag{1}$$

where S_i^t is agent i's state at time t and S_j^t is a neighboring agent's state. This measures how much knowing a neighbor's current state reduces uncertainty about the focal agent's next state, beyond what the agent's own current state provides.

Miller-Madow bias correction is applied. For the top-50 rules in each condition, median TE values are: Phase 2 = 0.072 bits, Phase 1 = 0.003 bits, Control = 0.113 bits. Phase 2 shows substantially elevated TE compared to Phase 1, confirming directional information flow from neighbors to agents. The Control condition's higher TE reflects its inclusion of a step-clock dimension that creates temporal state dependence without genuine spatial coordination (recall that Control $\mathrm{MI}_{\mathrm{excess}} \approx 0$).

Capacity-Matched Controls

To further isolate the role of observation content from table capacity, we evaluated two additional control conditions:

- Capacity-matched Phase 1: 100-entry tables where indices are aliased so that all dominant-state values for the same (self-state, neighbor-count) pair map to the same action. This provides Phase-2-sized tables with only Phase-1-level observation content.
- Random-encoding Phase 2: 100-entry tables with the same alphabet size as Phase 2, but the mapping from neighborhood configuration to observation index is randomly permuted. This tests whether the structure of the encoding matters beyond alphabet size.

The capacity-matched Phase 1 control produces median $\mathrm{MI}_{\mathrm{excess}} = 0.000$ (survival 71.4%), matching standard Phase 1 ($\mathrm{MI}_{\mathrm{excess}} = 0.000$) and well below standard Phase 2 ($\mathrm{MI}_{\mathrm{excess}} = 0.096$). This confirms that table capacity alone does not explain the Phase 2 advantage—Phase-1-level observations remain ineffective even with 100-entry tables. The random-encoding Phase 2 control produces median $\mathrm{MI}_{\mathrm{excess}} = 0.106$ (survival 75.1%), comparable to standard Phase 2, which is

expected because the observation encoding (self-state, neighbor count, dominant state) is identical; only the table-entry ordering differs, which is irrelevant for randomly generated tables.

Space-Time Plots

Space-time plots (kymographs) for representative rules from each condition are available in the code repository. These show the temporal evolution of agent states on the grid, providing qualitative visual evidence for the distinct dynamical regimes described in the main text: Phase 1's frozen crystallization, Phase 2's sustained dynamic coordination, and Control's chaotic fluctuations.

Algorithmic Pseudocode

Simulation loop (world.py:step()). At each of the 200 time steps:

1. Generate a random permutation of agent indices.
2. For each agent in order:
   (a) Observe local neighborhood (von Neumann, 4 cells).
   (b) Compute observation vector (s, n, d) or (s, n) depending on phase, where s = own state, n = occupied neighbor count, d = dominant neighbor state.
   (c) Look up action in shared rule table: $a = T[\text{index}(s, n, d)]$.
   (d) Execute action: move (if target cell empty), change state, or no-op.

Filter checks (filters.py). After each step, check: (1) Halt: positions and states unchanged for 10 consecutive steps $\rightarrow$ terminate. (2) State uniform: all agents share the same state $\rightarrow$ terminate.

MI computation (metrics.py). For the final snapshot:

1. Enumerate all occupied neighbor pairs (right/down on torus, deduped).
2. Compute joint and marginal state distributions from pairs.
3. $\hat{I} = \sum p(s_i, s_j) \log_2 \frac{p(s_i, s_j)}{p(s_i)\, p(s_j)}$.
4. Apply Miller-Madow correction: $\hat{I}_{\text{MM}} = \hat{I} - \frac{K_{\text{joint}} - K_X - K_Y + 1}{2n \ln 2}$.
5. Clamp to ≥ 0.

Shuffle null (metrics.py). Repeat 200 times: permute states among fixed occupied positions, compute $\hat{I}_{\text{MM}}$, average. $\text{MI}_{\text{excess}} = \max(\hat{I}_{\text{MM}} - \overline{I}_{\text{shuffle}}, 0)$.

References